Science of the Total Environment 755 (2021) 142634

Contents lists available at ScienceDirect

Science of the Total Environment

journal homepage: www.elsevier.com/locate/scitotenv

The US COVID-19 pandemic in the flood season

Xinyi Shen [a,*], Chenkai Cai [a,b,1], Qing Yang [a,c,1], Emmanouil N. Anagnostou [a], Hui Li [d]

[a] Department of Civil and Environmental Engineering, University of Connecticut, Storrs, CT 06269, United States of America
[b] College of Hydrology and Water Resources, Hohai University, Nanjing 210098, China
[c] College of Civil Engineering and Architecture, Guangxi University, Nanning, Guangxi 530004, China
[d] Department of Finance, University of Connecticut, Storrs, CT 06269, United States of America

ARTICLE INFO

Article history:
Received 6 August 2020
Received in revised form 25 September 2020
Accepted 26 September 2020
Available online 1 October 2020

Editor: Jay Gan

Keywords:
COVID-19
Flood
Displacement
Compound Natural Hazard

ABSTRACT

Flooding displaces large populations each season, which potentially increases the exposure of the vulnerable societies. Having failed to curve down the number of people infected with COVID-19 in the first wave of the pandemic, many states in the United States (U.S.) are now at high risk of the concurrence of the two disasters. Assessing this compound risk before the country enters the flood season is of vital importance. Therefore, we provide a prompt tool to assess the compound risk of COVID-19 at the county level over the U.S. We find that (1) the number of flood insurance house claims can proxy the displaced population accurately with more spatiotemporal detail, and (2) the high-risk areas of both flooding and COVID-19 are concentrated along the southern and eastern coasts and some parts of the Mississippi River. Our findings may trigger the interest of further exploring the topics related to the concurrence of COVID-19 and flooding.

1. Introduction

As of July 2020, the COVID-19 global pandemic had infected more than four million population in the United States (U.S.). In Wuhan, where the virus was first reported, the initial reproductive number (R_0) was 2.2 (Li et al., 2020), it has been up to 6.5 globally (Liu et al., 2020). In the U.S., which is seeing the record-breaking numbers of infections following a reckless reopening of states (Knauer, 2020), the best-case outcome in the absence of a vaccine or effective has proved to be managing a controlled transition from community spread. Nonpharmaceutical mitigation measures including social distancing and have been proved effective in curving the number of infectees (Anderson et al., 2020; Dehning et al., 2020; Lai et al., 2020; Prem et al., 2020; Shen et al., 2020). This has left the U.S. successfully in bending the curve, just as the country is about to enter the flood season.

During the past three years, flooding alone has displaced 10,729 people per year on average in the U.S. (Internal Displacement Monitoring Centre, IDMC, https://www.internal-displacement.org/countries/united-states). This year, potentially increased exposure of the flood-displaced population to COVID-19 may yield a greater risk of infection. Flood risk is traditionally evaluated by hydrological models (Fu et al., 2014; Liang et al., 1994; Shen and Anagnostou, 2017; Shen et al., 2016), sometimes coupled with hydraulic models (Bates et al., 2010; Hardesty et al., 2018; Yamazaki et al., 2011) at global, national, and local scales in terms of the output discharge, inundation extent (Shen et al., 2019a; Shen et al., 2019b), or depth (Cohen et al., 2017). The traditional flood risk measures cannot, however, be linked directly to the displaced population.

Moreover, while many published studies have analyzed the risk of either flooding or COVID-19, none has evaluated the compound risk posed by the concurrence of the two. In this study, we aim to provide a prompt tool to overview the compound risk before the flood season by utilizing three datasets, 10 years of flood insurance house claims (referred to as flood claims hereafter), the displaced population from the past three years, and the COVID-19 infectee records. We will process the final result to the county level over the U.S.

2. Materials and methods

2.1. COVID-19 transmissivity

Since May 22, many states have reopened regardless of the ongoing pandemic. We use the mean daily reproductive number from May 22 to

* Corresponding author.
E-mail address: xinyi.shen@uconn.edu (X. Shen).
[1] Co-first author

https://doi.org/10.1016/j.scitotenv.2020.142634
0048-9697/

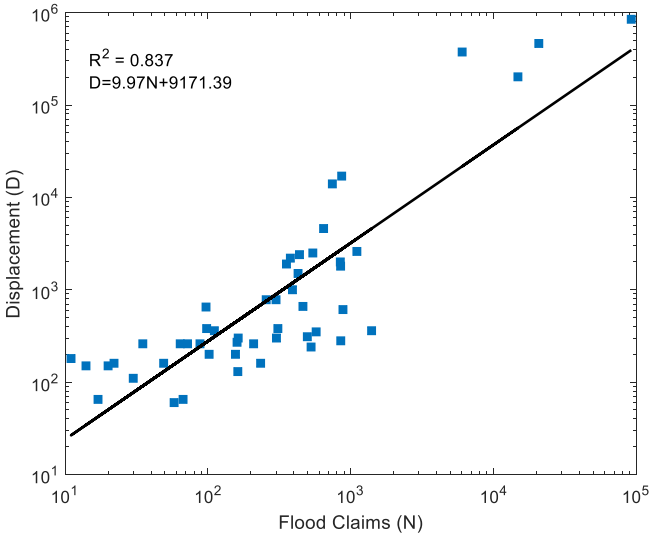

Fig. 1. Scatter plots of displaced population and flood claims (N) during flood events since 2017 over the U.S. National Flood Insurance Program NFIP Gridded flood claims are aggregated to match the spatiotemporal range of the displacement data (D) by Internal Displacement Monitoring Centre (IDMC).

July 1 to represent the current risk of COVID-19. The reproductive number, R_0, is defined as the average number of secondary infectees generated by a primary infector (Van den Driessche and Watmough, 2008). Therefore, we define a greater than unity R_0 as representing moderate to extremely high risk and a smaller than unity R_0 as indicating low risk.

2.2. Reproductive number estimation

We employ a stochastic approach (Flaxman et al., 2020) to estimate the reproductive number, R_0 from the clinical confirmation of COVID-19 infectees assembled at Johns Hopkins University (Dong et al., 2020). The approach models as discrete stochastic number of days the time delay from when a person becomes infected to his/her clinical confirmation as a discrete stochastic number of days, and the time from when a person gets infected and to when he/she infects another person. Then the R_0 of a given county on day t, R_{0t}, can be estimated from the daily confirmed number of infectees (C), via an intermediate variable, the daily number of new infectors (I). The conversion from C_t to I_t is given by Eq. (1),

$$I_t = \sum_{\tau=t+1}^{t+N} C_\tau lgn_{\tau-t} \quad (1)$$

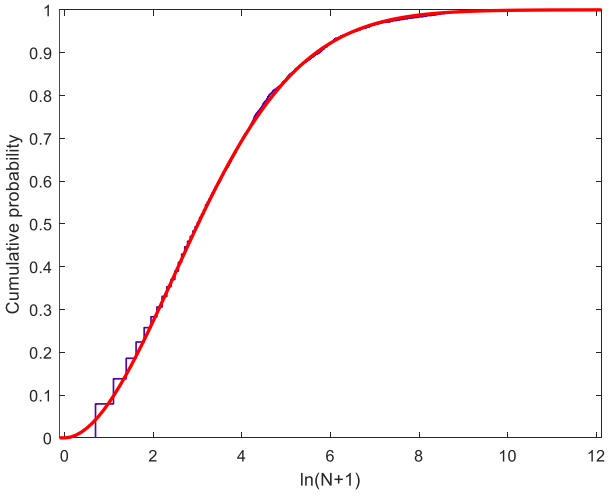

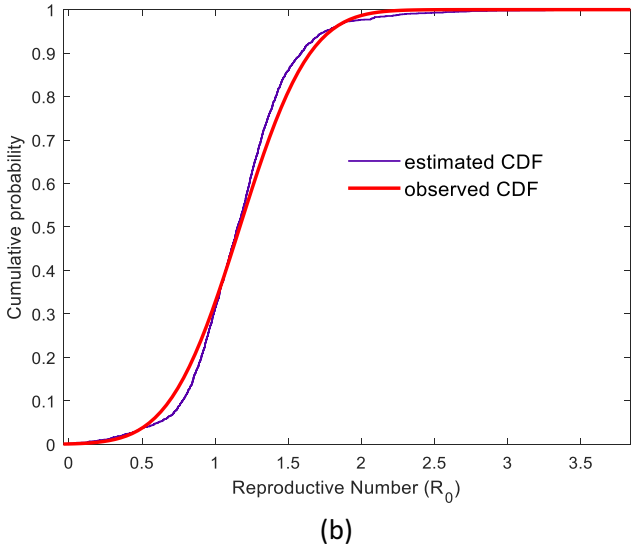

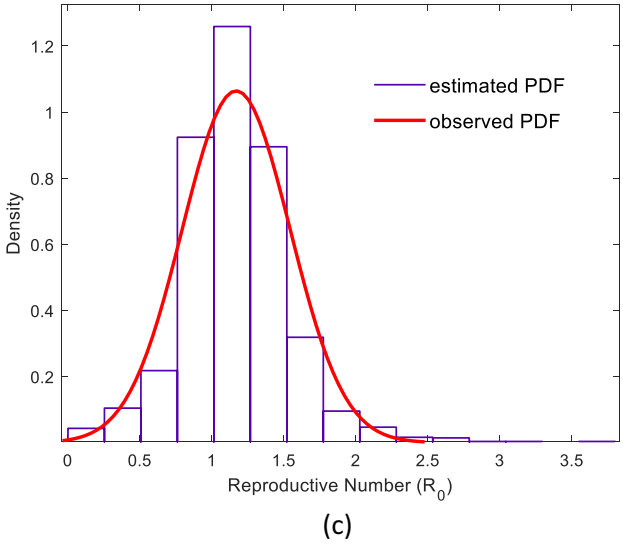

Fig. 2. Distribution of flood claims (a) and the reproductive number of COVID-19 (b) and (c).

Table 1
Classification standard of R_0 and positive flood claim. N represents the number of positive flood claims, Q represents the CDF of the standard normal distribution, and Q^{-1} is its inverse.

Standardized magnitude	R_0	N
Low	$R_0<1$	$Q^{-1}(N) < 0$
Medium	$R_0 \geq 1$ *and* $Q^{-1}(R_0) < 0.5$	$0 \leq Q^{-1}(N) < 1$
High	$0.5 \leq Q^{-1}(R_0) < 1.5$	$1 \leq Q^{-1}(N) < 2$
Very high	$Q^{-1}(R_0) \geq 1.5$	$Q^{-1}(N) \geq 2$

where lgn_t is the probability of an infectee's receiving clinical confirmation t days since being infected (Lauer et al., 2020). Note that in Eq. (1), C records with a 14-day extension need to be used to estimate the I_t on a given day. Therefore, we use the COVID-19 records until July 15 to study the period up to July 1. The conversion from I_t to R_{0t} is given by Eq. (2),

$$R_{0t} = I_t / \sum_{\tau=t-N}^{t-1} I_\tau g_{t-\tau} \quad (2)$$

where g_t is the probability of an infector's infecting other people on the day t since being infected.

2.3. Invalid R_0 value trimming

Non-local community spread can occur in two situations in a given response unit: before the community spread starts, or when a large number of infectors are imported in the middle of a community spread. Both situations could result in an erroneous R_0 value. For the first situation, we simply set 30 accumulated cases as the minimum threshold for a community spread to start. R_0 outside of the community spreading period will be set as No Data. The second situation is featured by a sharp peak of daily confirmed infectees and/or many days of zero newly confirmed cases. In this situation on a given day, if either the number of newly confirmed infectees on the given day is at least 10 times of any other day within the 14-day window the given day is centered in, or the number of newly confirmed infectees are zero on no less than 4 days in the 14-day window ending on the given day, we set R_0 of the 14-day window ending on the given day as No Data.

2.4. Flood claims and displaced population

The National Flood Insurance Program (NFIP) provides records of flooded claims (N) and policies since 1972, with the location precise to 0.1 × 0.1° (~10 km) (https://www.fema.gov/media-library/assets/documents/180374). We hypothesize that the displaced population is strongly correlated to the number of flood claims. To verify, we aggregate the gridded flood claim number N to match the spatiotemporal range of the IDMC records; then compute the Pearson correlation coefficient (r) between the aggregated flood claims and the displaced population available at IDMC since 2017. The high correlation ($r^2 = 0.83$), as shown in Fig. 1, justifies the use of flood claims instead of the displaced population because the former (NFIP records) have more spatial detail and longer records. Finally, we use the total NFIP flood claims at the county level from 2010 to 2019 to represent the flood risk.

2.5. The compound risk characterization

We find the Normal and Weibull distributions could well characterize the county-level R_0 and positive claims (see Fig. 2), as written by Eqs. (3) and (4), and they have low correlation ($r = 0.09$). Therefore, we standardize each marginal risk to low, moderate, high, and very high, then composite the two-dimensional risks as the compound one. Note that when the R_0 is smaller than unity, the virus is likely to die out. Therefore, we define the low COVID-19 risk category as $R_0 < 1$. The standardized thresholds for other categories are listed in Table 1. Note that although we attempt to remove erroneous R_0 values by implementing a trimming algorithm, the lack of tests at early stages or the insufficient test capabilities in some counties can still bias the transmissivity estimation (Manski and Molinari, 2020). Therefore, the standardization might characterize the risk of COVID-19 more accurately than directly using the reproductive number.

$$R_0 \sim N(1.17, 0.37) \quad (3)$$

$$\ln(N+1) \sim Weibull(3.26, 1.65) \quad (4)$$

3. Results

Compositing the flood and COVID-19 risks at the county level over the U.S. reveals the hotspots of the compound risk and each marginal

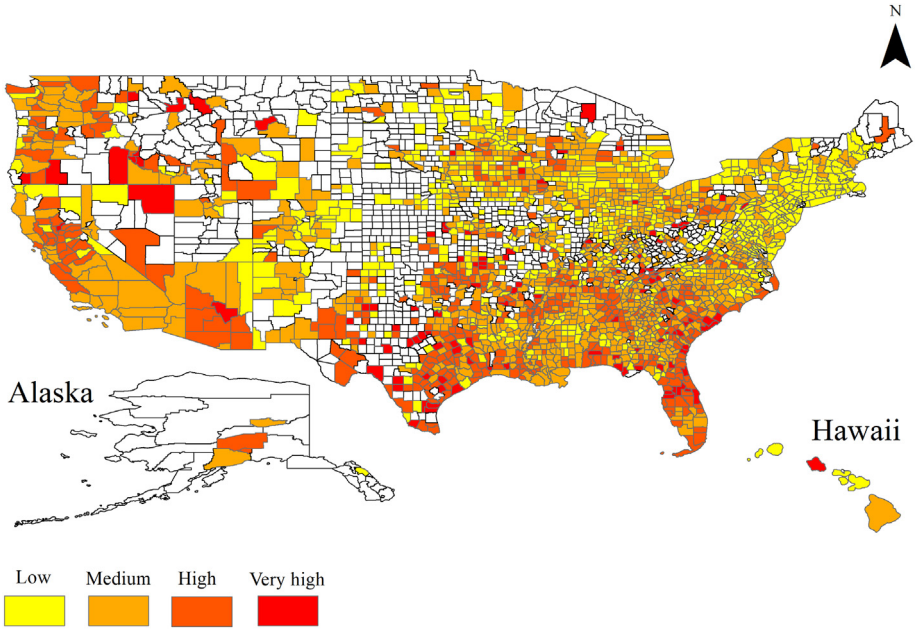

Fig. 3. Mean daily R_0 from May 22 to July 1, 2020 at county-level. Blank counties either have no data or very short period of valid records of community spread in the time window.

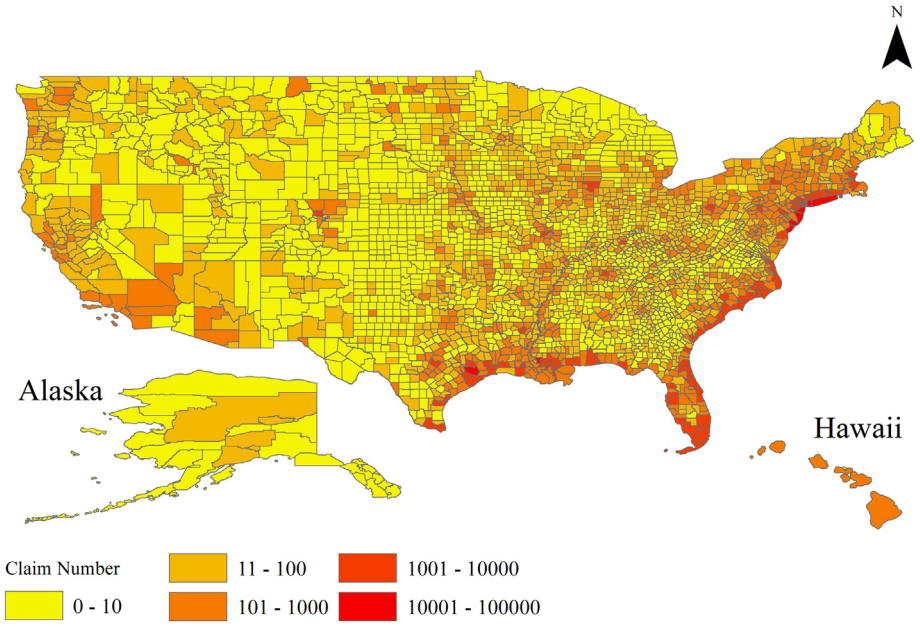

Fig. 4. Accumulated flood claims from 2010 to 2019 at the county level.

risk. Although the correlation between the historical flood risk and recent COVID-19 risk is low, areas at high risk for both exist. As shown in Fig. 3, the US COVID-19 capitals include the west coastal, south coastal, and southeastern coastal counties, and the south great plains. Fig. 4 shows the flood risk is relative higher along the southern and eastern coasts, and in areas along the Mississippi River and its main branches. Consequently, the compound risk is equal or above the high level (for both) along the southern and eastern coastal counties and some part of the Mississippi River, as shown in Fig. 5.

4. Discussion

We present a prompt tool to estimate the compound risk posed by flooding and COVID-19. The areas of high risk for both types of hazards are concentrated along southern and eastern coastal states, and along the Mississippi River and its main branches. We also note that although the northeastern coast used to be the capital of COVID-19 and is also at high risk for flooding, the compound risk is no thigh because the COVID-19 risk is currently low. The latter can be attributed to the effective and

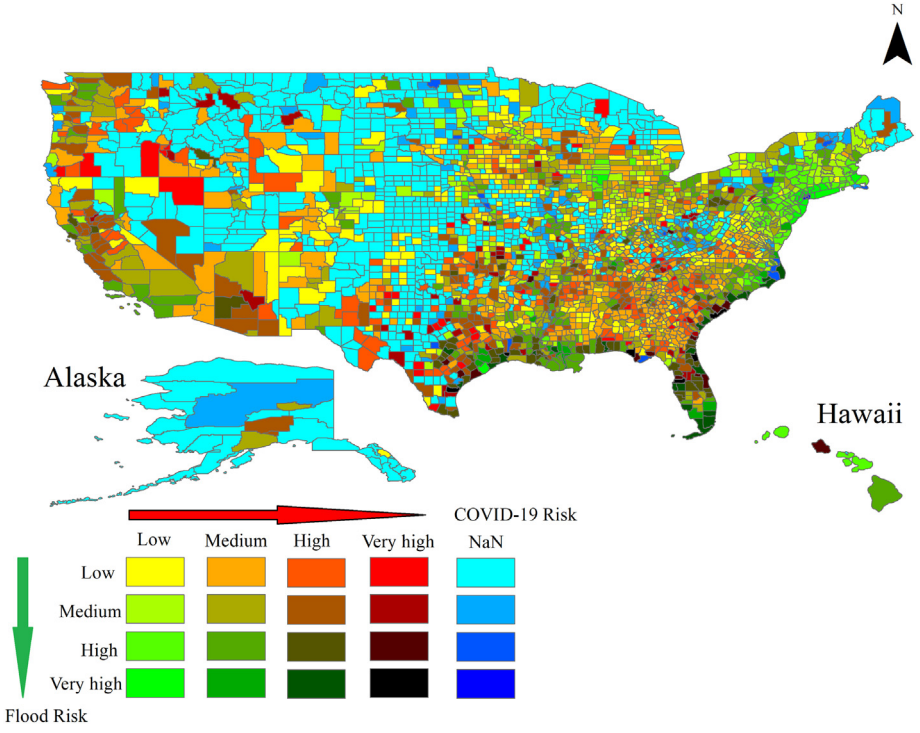

Fig. 5. The compound risk of flooding and COVID-19.

stringent mitigation policies adopted by these states (e.g., New York state, especially New York City). Note that the insufficient COVID-19 clinical records available for many midwestern counties for the period of consideration could make the evaluation of COVID-19 risk less accurate there. Furthermore, it worth noting that in areas frequently that experience flooding, residents might be more prepared than areas with less frequent flooding, resulting a different relationship of flood severity and impact than we expect before the flood season.

Our study may trigger the interest of studying the following topics: (1) predicting the flood risk or COVID-19 risk for the next season; and (2) physically estimating the feedback from flood damage to COVID-19 risk (e.g., the transmissivity) in 2020 or parameterizing the flood damage in modeling the COVID-19 risk.

Declaration of competing interest

The authors declare no conflict of interest.

Acknowledgment

We want to give many thanks to Dr. Lisa Ferraro Parmelee (LFP Editorial Enterprises LLC) for the professional proofreading of this manuscript during her vacation time, and the editorial board of *Science of the Total Environment* for the prompt processing, which ensures the timely submission and processing of this COVID-19 related manuscript.

References

Anderson, R.M., Heesterbeek, H., Klinkenberg, D., Hollingsworth, T.D.J.T.L., 2020. How will country-based mitigation measures influence the course of the COVID-19 epidemic? Lancet 395, 931–934. https://doi.org/10.1016/S0140-6736(20)30567-5.

Bates, P.D., Horritt, M.S., Fewtrell, T., 2010. A simple inertial formulation of the shallow water equations for efficient two-dimensional flood inundation modelling. J. Hydrol. 387, 33–45. https://doi.org/10.1016/j.jhydrol.2010.03.027.

Cohen, S., Brakenridge, G.R., Kettner, A., Bates, B., Nelson, J., McDonald, R., et al., 2017. Estimating floodwater depths from flood inundation maps and topography. JAWRA J. Am. Water Resour. Assoc. https://doi.org/10.1111/1752-1688.12609.

Dehning, J., Zierenberg, J., Spitzner, F.P., Wibral, M., Neto, J.P., Wilczek, M., et al., 2020. Inferring change points in the spread of COVID-19 reveals the effectiveness of interventions. Science https://doi.org/10.1126/science.abb9789.

Dong, E., Du, H., Gardner, L., 2020. An interactive web-based dashboard to track COVID-19 in real time. Lancet Infect. Dis. 20. https://doi.org/10.1016/S1473-3099(20)30120-1.

Flaxman, S., Mishra, S., Gandy, A., Unwin, H.J.T., Mellan, T.A., Coupland, H., et al., 2020. Estimating the effects of non-pharmaceutical interventions on COVID-19 in Europe. Nature https://doi.org/10.1038/s41586-020-2405-7.

Fu, C., James, A.L., Yao, H., 2014. SWAT-CS: revision and testing of SWAT for Canadian Shield catchments. J. Hydrol. 511, 719–735. https://doi.org/10.1016/j.jhydrol.2014.02.023.

Hardesty, S., Shen, X., Nikolopoulos, E., Anagnostou, E., 2018. A numerical framework for evaluating flood inundation risk under different dam operation scenarios. Water 10. https://doi.org/10.3390/w10121798.

Knauer, N.J., 2020. The COVID-19 pandemic and federalism. SSRN 3599239. https://doi.org/10.2139/ssrn.3599239.

Lai, S., Ruktanonchai, N.W., Zhou, L., Prosper, O., Luo, W., Floyd, J.R., et al., 2020. Effect of non-pharmaceutical interventions to contain COVID-19 in China. Nature https://doi.org/10.1038/s41586-020-2293-x in press.

Lauer, S.A., Grantz, K.H., Bi, Q., Jones, F.K., Zheng, Q., Meredith, H.R., et al., 2020. The incubation period of coronavirus disease 2019 (COVID-19) from publicly reported confirmed cases: estimation and application. Ann. Intern. Med. 172. https://doi.org/10.7326/M20-0504.

Li, Q., Guan, X., Wu, P., Wang, X., Zhou, L., Tong, Y., et al., 2020. Early transmission dynamics in Wuhan, China, of novel coronavirus–infected pneumonia. N. Engl. J. Med. https://doi.org/10.1056/NEJMoa2001316.

Liang, X., Lettenmaier, D.P., Wood, E.F., Burges, S.J., 1994. A simple hydrologically based model of land surface water and energy fluxes for general circulation models. Journal of Geophysical Research: Atmospheres 1984–2012 (99), 14415–14428. https://doi.org/10.1029/94JD00483.

Liu, Y., Gayle, A.A., Wilder-Smith, A., Rocklöv, J., 2020. The reproductive number of COVID-19 is higher compared to SARS coronavirus. J. Travel Med. 27. https://doi.org/10.1093/jtm/taaa021.

Manski, C.F., Molinari, F., 2020. Estimating the COVID-19 infection rate: anatomy of an inference problem. J. Econ. https://doi.org/10.1016/j.jeconom.2020.04.041 in press.

Prem, K., Liu, Y., Russell, T.W., Kucharski, A.J., Eggo, R.M., Davies, N., et al., 2020. The effect of control strategies to reduce social mixing on outcomes of the COVID-19 epidemic in Wuhan, China: a modelling study. Lancet Public Health https://doi.org/10.1016/S2468-2667(20)30073-6.

Shen, X., Anagnostou, E.N., 2017. A framework to improve hyper-resolution hydrologic simulation in snow-affected regions. J. Hydrol. 552, 1–12. https://doi.org/10.1016/j.jhydrol.2017.05.048.

Shen, X., Hong, Y., Zhang, K., Hao, Z., 2016. Refining a distributed linear reservoir routing method to improve performance of the CREST model. J. Hydrol. Eng. 04016061. https://doi.org/10.1061/(ASCE)HE.1943-5584.0001442.

Shen, X., Anagnostou, E.N., Allen, G.H., Brakenridge, G.R., Kettner, A.J., 2019a. Near real-time nonobstructed flood inundation mapping by synthetic aperture radar. Remote Sens. Environ. 221, 302–335. https://doi.org/10.1016/j.rse.2018.11.008.

Shen, X., Wang, D., Mao, K., Anagnostou, E., Hong, Y., 2019b. Inundation extent mapping by synthetic aperture radar: a review. Remote Sens. 11, 879. https://doi.org/10.3390/rs11070879.

Shen, X., Cai, C., Li, H., 2020. Socioeconomic restrictions slowdown COVID-19 far more effectively than favorable weather-evidence from the satellite. Sci. Total Environ. 141401. https://doi.org/10.1016/j.scitotenv.2020.141401.

Van den Driessche, P., Watmough, J., 2008. Further notes on the basic reproduction number. In: Brauer, F., van den Driessche, P., Wu, J. (Eds.), Mathematical Epidemiology. 1945. Springer, Berlin, Heidelberg, pp. 159–178.

Yamazaki, D., Kanae, S., Kim, H., Oki, T., 2011. A physically based description of floodplain inundation dynamics in a global river routing model. Water Resour. Res. 47, W04501. https://doi.org/10.1029/2010WR009726.